TRACE: Detection of Permeable Deep-Reaching Fault Zone Sections in the Upper Rhine Graben, Germany, During Low-Budget Isotope-Geochemical Surface Exploration

Michael Kraml[1], Marco Jodocy[1], John Reinecker[1], Dominique Leible[1], Florian Freundt[2], Sami Al Najem[3], Gerhard Schmidt[3], Werner Aeschbach[2], and Margot Isenbeck-Schroeter[3]

[1] GeoThermal Engineering GmbH, Karlsruhe, Germany

[2] Institute of Environmental Physics, Heidelberg University, Heidelberg, Germany

[3] Institute of Earth Sciences, Heidelberg University, Heidelberg, Germany

kraml@geo-t.de

Keywords: Isotope geochemistry, fault zone permeability, Upper Rhine Graben.

ABSTRACT

Due to the apparent lack of surface manifestations (blind resources), current methods of geothermal surface exploration in Germany rely on expensive geophysical methods (mainly 3D reflection seismic surveys) to identify the geometry of hydrogeothermal low-temperature aquifers and permeable fault zones in depth. However, geophysics alone do not allow for an estimation of present-day's fault permeability nor provide a characterization of the chemical properties of the local deep aquifer fluid. Both factors are important for optimising siting of geothermal wells to obtain maximum flow rates and sustainable operation of a binary power plant.

The TRACE project, funded by the Federal Ministry for Economic Affairs and Energy (funding code FKZ: 0325390), presents a low-cost strategy for characterizing deep hydrogeothermal reservoirs using a combination of methods from hydrogeochemistry and isotope geochemistry on fluid samples mainly taken from shallow groundwater wells. The main goal is to confine the area of interest for further geophysical investigation, as already done in the exploration of high-temperature resources around the world. For this purpose naturally occurring geochemical and isotopic tracers like noble gases, and radiogenic isotopes of strontium and lithium are investigated.

The Upper Rhine Graben was chosen to test the multi-tracer method due to its well-studied geology and some significant pre-existing geophysical exploration data which allow for validation of the study's findings.

The project's objective was to identify the most useful tracers of deep geothermal fluid circulation, which consecutively can be applied to other regions with less prior information.

The new surface exploration data from the Northern Upper Rhine Graben close to Groß-Gerau, Germany, show promising results, indicating fault sections of increased permeability where elevated helium and strontium isotope ratios coincide with specific geochemical characteristics, fault traces and a previously known saltwater anomaly in the shallow groundwater.

These findings are in accordance with independent geomechanical modelling. The modelling results display zones of enhanced structural permeability for upwelling thermal fluids as indicated by an enhanced slip and dilation tendency in the same section of the fault characterized by enhanced mantle helium and chloride concentrations.

The most likely reason for deep fluid pathways are (i) the mantle shear zone (detected by refraction seismics) persisting through the lower crust and (ii) diatreme pipes etc. to channel mantle fluids to a level of enhanced structural permeability in the upper crust.

1. INTRODUCTION TO THE STUDY AREA

The study area is located in the Northern Upper Rhine Graben (URG) >10 km southwest of Frankfurt Airport (Figure 1). The western boundary of the geothermal license area (owned by municipal utility 'Überlandwerk Groß-Gerau GmbH') is following the Western Master Fault (WMF) of the URG. The Quaternary groundwater aquifer is >100 m thick with major exception of the Western Lower Main Valley (i.e. <10 m thickness at the northern sampling sites of Bad Weilbach). All groundwater samples were taken from monitoring and production wells within the uppermost ~10 m of the shallowest aquifer. The strategy of a sampling array in the shallowest aquifer was chosen because of a known salt water anomaly reaching to the near surface level (Schmitt & Steuer 1974; Siemon et al. 2001 and references therein).

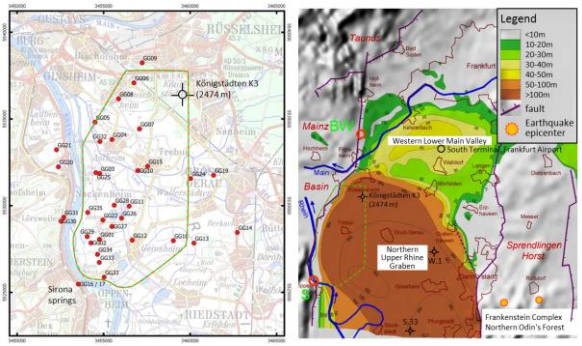

Figure 1: Thickness of the Quaternary aquifer (Röhr: http://www.oberrheingraben.de), epi-centres of major earthquakes in 2014 (Homuth et al. 2014), licence area, location of deep oil wells, and sampling locations (S = Sirona springs; BW = Bad Weilbach wells). W.1 = Weiterstadt 1 and S.33 = Stockstadt 33 oil wells both reaching the basement.

The structural framework in the working area is characterized by a relay ramp and the major structures were revealed via 2D seismic surveys during former hydrocarbon exploration in that area (Figure 2).

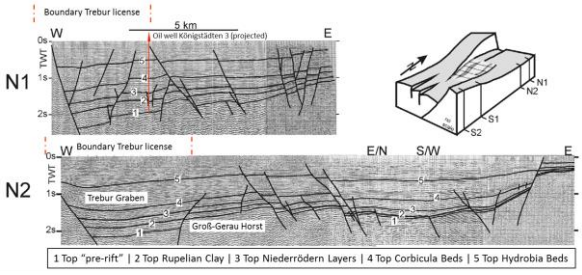

Figure 2: Major structures in the subsurface of the working area i.e. Trebur Graben and Groß-Gerau Horst as evident in 2D seismic lines (after Derer 2003).

The WMF is indicated at the earth's surface by the so called 'Nackenheim Swell' in the river bed and a copper mineralization (Figure 3) as well as by a groundwater cascade near Bauschheim and damages of buildings in the urban area of Rüsselsheim (Schmitt 1974), located further north.

Diatreme pipes and alkali-basalt occurrences are of special interest concerning potential conduits for mantle gases (Figure 3). During 3D seismic data evaluation another maar was recently discovered in the subsurface of the working area (Lutz et al. 2016, in prep.).

Historic seismicity in the northern URG also occurs in form of earthquake 'swarms' (Homuth et al. 2014, Landsberg 1931). The epicentres of the strongest events (M=4) of the most recent activity in 2014 are shown in Figure 1 (Homuth et al. 2014).

Surface manifestations of hydrothermal activity in the subsurface are rare and usually not considered in surface exploration of German geothermal prospects. However, a part of the study area is characterized by salt-tolerant plants (Böger 1985), a higher number of electro-fished salt-tolerant eel in little tributary rivers (Korte et al. 2007) and occurrences of salty water in a few meters depth of groundwater wells (TDS up to 6.7g/l; Carlé 1975). Additional to the nowadays upwelling deep saline fluid, a copper sulphide mineralization and related gangue calcite also indicates the hydraulically active section of the WMF at the time interval of their formation (Figure 3).

In contrast to the central and southern URG, Tertiary salt deposits (anhydrite and halite which could be relevant for fluid evolution) occur in the northern URG only in the upper Oligocene i.e. mid-Cerithia beds (Schäfer 2012).

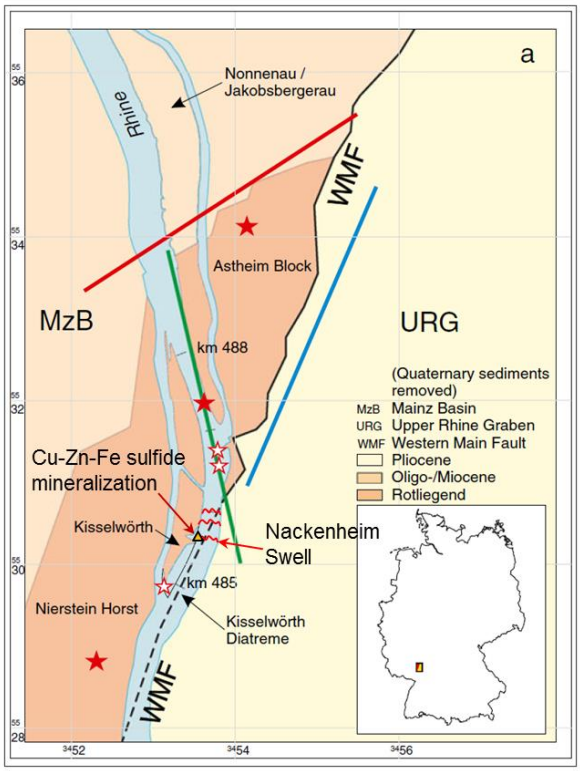

Figure 3: Location of diatremes (white stars with red rim) and alkali-basalt occurrences (red stars). The colored lines show the major strike directions of the local fault pattern (Lutz et al. 2013). The sulfide mineralization and swell at the WMF (Schmitt & Steuer 1974) are also shown.

The magma injections related to graben formation (e.g. dated Kisselwörth diatreme: 55.8 ± 0.2 Ma; Lutz et al. 2013) and the nearby fossil (undated) mineralization (Figure 3) in low-permeable country rocks (= Permian sediments of the Nierstein Horst) are prominent indicators for a long (at least episodic) permeability history of that part of the WMF.

The basement in the northern part of the study area close to the Taunus border fault (Rheic suture) consists of phyllites (Northern Phyllite Zone), whereas the basement in the major part of the working area is made of rocks of the mid-German crystalline rise i.e. granodiorite plus minor amphibolites (Schwabe &

Scheibe 2012). The amphibolites are more abundant to the west or a gabbro is present in the westernmost part of the working area as revealed by 3D gravity modeling (Schwabe & Scheibe 2012).

2. RESULTS

The data tables of the analytical results and the description of the applied analytical methods are presented and described in detail by Al Najem et al. 2016, Schmidt et al. 2016, Freundt et al. 2015.

2.1 Water chemistry

The major element composition is shown in Figure 4. Near-surface groundwater component 1 is controlled by the lithology of the Quaternary aquifer. Component 1 is similar in composition to sample GG33, which is also characterized by the lowest Sr isotope ratio (see below), and mixed with the uprising saline deep fluid (component 2 most closely approximated by sample GG26). Deep component 2 is represented by fossil seawater (connate water) of the basinal brine in the basement. The study area was most recently flooded by seawater in mid-Oligocene (e.g. Schäfer 2012) which allowed an infiltration of seawater via faults into the basement of the URG which subsided since Eocene.

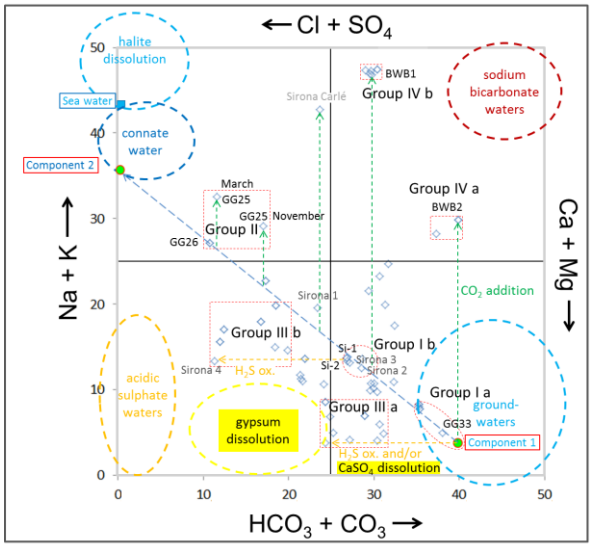

Figure 4: Ludwig-Langelier diagram with analytical results including an additional analysis of Carlé (1975) and 4 analyses of GRUSCHU data base for Sirona 1-4 spring (http://gruschu.hessen.de/). Encircled water types (stippled lines) are based on Vaselli et al. (2002).

Additional to mixing with mobilized fossil seawater, two further processes have taken place in fluid evolution: CO_2 addition and H_2S oxidation (Figure 4). The samples of group 3a could have evolved from waters of group 1a by $CaSO_4$ dissolution or H_2S oxidation. In contrast, the sulfate-richer waters of group 3b can only derive from group 1b (containing most of the Sirona spring analyses) via H_2S oxidation. The monitoring wells of group 3b are situated downstream of well GG26 in groundwater flow direction.

The water composition of sulfur 'spring' Bad Weilbach 2 (BWB2; group 4a) is derived from group 1a via interaction with CO_2. Na-Li 'spring' Bad Weilbach 1 (BWB1, group 4b) is explained by CO_2 uptake of group 1b waters. The latter are characterized by admixture of minor connate water. The role of CO_2 in evolution of group 4a,b waters is supported by high concentrations of free CO_2 found in both Bad Weilbach 'springs' (Carlé, 1975).

In this context it is remarkable that also other samples (e.g. the dried up Sirona sulfur spring [Carlé 1975] and GG25), which are taken at locations situated at the WMF, are influenced by CO_2. Therefore, it is most likely that the CO_2 is ascending at the WMF and interacts with the saline fluids. Future carbon isotope analyses will show whether the CO_2 is mantle derived or not.

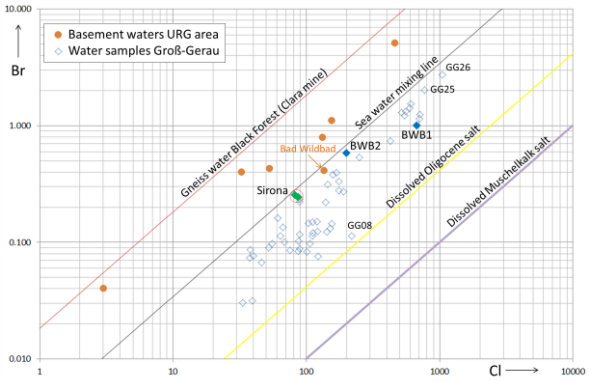

Figure 5: Br-Cl diagram with analytical results (rhombic symbols) and additional analyses of basement waters (brown dots; Bucher & Stober 2010). Mean value of gneiss water (Clara mine) from Bucher et al. (2009) and dissolved Oligocene and Middle Triassic salt from Stober & Bucher (1999).

The saline component 2 can be characterized e.g. by the Cl/Br ratio (Figure 5). Figure 5 shows that all groundwater samples could contain a more or less significant saline component from Oligocene salt which is widely present in the basement (infiltrated during transgression as described above). Only the Sirona springs and BWB2 waters of Bad Weilbach sulfur 'spring' could have derived their salinity solely from water-rock interaction with the silicate rocks of the basement if the basement below the study area is similar to that of Bad Wildbad in the Black Forest (brown dot) in respect to the Cl/Br ratio.

Please note that halite coatings on silicate minerals have even been found in basement rocks of the lower crust (Markl & Bucher 1998) and that most likely also vein fillings of anhydrite exist in the basement (Bucher & Stober 2010).

Additional to the major solutes also trace elements including rare earth elements (REE) were analyzed

(Al Najem et al. 2016). Chondrite normalized REE pattern either revealed a negative europium (Eu) anomaly as expected for cold surface waters of the upper crust (McLennan 1989) or no Eu anomaly.

Most samples characterized by oxidizing conditions show – as expected – a more or less pronounced negative cerium (Ce) anomaly. Solely sample GG26 shows a well pronounced gadolinium (Gd) anomaly (Figure 6). This sample is also characterized by the highest mantle helium concentration of the analyzed ground waters.

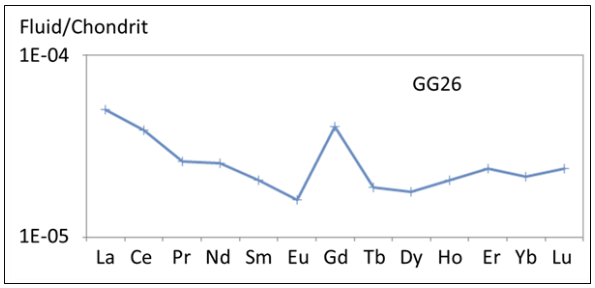

Figure 6: REE pattern of sample GG26 with the only pronounced positive Gd anomaly.

The reason whether the Gd anomaly is caused by ascending deep fluid or not is subject to further studies which could exclude an anthropogenic contamination (e.g. Kulaksız & Bau 2007). A geogenic source is currently favored since all neighboring groundwater wells do not show the Gd anomaly.

2.2 Radiogenic isotopic composition

The Sr isotopic composition of the groundwater in the study area is more radiogenic the closer the sample was taken at the WMF (Schmidt et al. 2016). Additionally, an apparent correlation of samples in the study area occurs concerning the saline upwelling fluids with the hot/mineralized springs emanating at Taunus boundary fault (Figure 7). In case such a direct hydraulic connection via permeable faults would exist, both Bad Weilbach 'springs' should plot on the same mixing line, because Bad Weilbach is situated between the study area *sensu stricto* and the Taunus mountains (Figure 1). However, there is no correlation of the Bad Weilbach samples with the other samples in the $^{87}Sr/^{86}Sr$ vs. 1/Sr diagram (Figure 7).

Additionally, the Taunus boundary fault is only permeable at short sections which were met by SE-NW striking faults of the Taunus mountains (Figure 13). Therefore, lateral fluid flow along the Taunus boundary fault is excluded.

In combination with the Li isotopic composition (Figure 8) it can be shown that the similarities between fluids of the Taunus boundary fault (TBF; Krontal samples) and Bad Weilbach (Na-Li 'spring') are caused by the same basement (phyllites) which occurs along their flow paths.

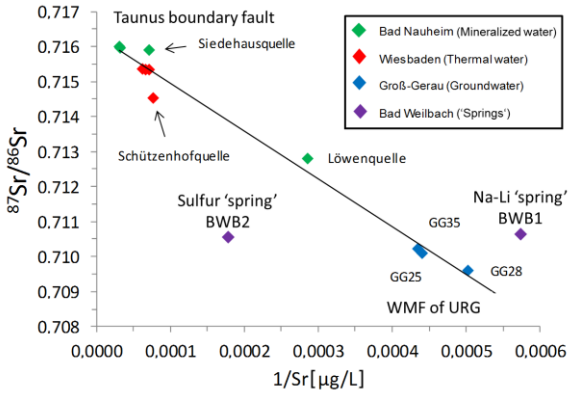

Figure 7: Strontium isotope ratio versus inverse Sr concentration (Schmidt et al. 2016).

In contrast the basement in the study area *sensu stricto* consists of (amphibolite-bearing) granodiorite which causes the differences in Li isotopic composition between Taunus and Bad Weilbach samples at one hand and the groundwater of the study area *sensu stricto* including the Sirona springs on the other hand (Figure 8).

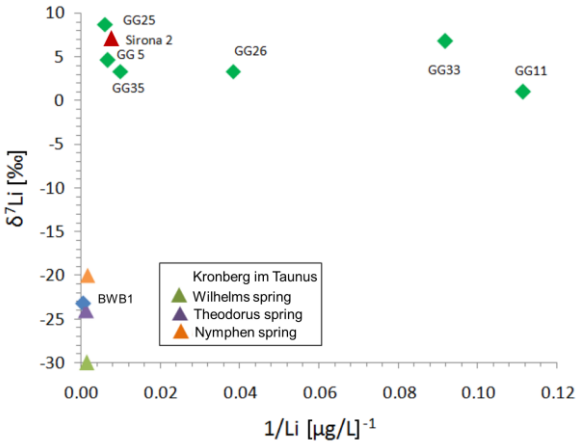

Figure 8: Lithium isotopic composition versus inverse Lithium concentration (Schmidt and Seitz, unpublished). Strongly negative δ^7Li values only occur in Bad Weilbach (Na-Li 'spring') at the northern section of the WMF and in Krontal at the Taunus boundary fault. The positive δ^7Li values of the 'Sirona spring group' are characteristic for the WMF in the south at Nierstein Horst (GG25, GG5, GG35) and further to the east. The latter groundwater samples (GG26, GG33, GG11) are more diluted (i.e. lower Lithium concentrations but same Lithium isotopic composition). (See text for further explanation).

Also the geochemical modeling could exclude that the deep upwelling fluid in the working area is similar in composition to the hot/mineralized springs emanating at the Taunus boundary fault (Al Najem et al. 2016).

2.3 Radon concentrations

Sirona spring in Nierstein and Na-Li 'spring' in Bad Weilbach (BWB1) are both situated at the WMF and are characterized by the highest measured radon (Rn) concentrations in the fluids of >20,000 Bq/m^3 and >10,000 Bq/m^3, respectively (Freundt et al. 2015).

Especially in case of Sirona spring, the fault reaches to the earth's surface without being covered by Quaternary unconsolidated sediments (Carlé 1975).

Also sample GG20 is characterised by a high Rn activity of >7.000 Bq/m^3 (Freundt et al. 2015). This sample was taken at the western boundary fault of the Nierstein Horst in a water well where the screen is located in the hard rocks of lower Tertiary age.

All further Rn water samples in the study area show lower activities between around 700 and 4,000 Bq/m^3 (Freundt et al. 2015). Only the sulfur spring of Bad Weilbach (BWB2) with almost 3,400 Bq/m^3 is in the same activity range than the near-surface groundwater. BWB2 (artesian outflow of 0.6 l/s) is situated on the hanging wall of the „Hattersheim Graben" and taps the western fault, which is the eastern boundary fault of the Mainz Basin. In contrast, BWB1 (artesian outflow of 1.4 l/s) is situated on the footwall and taps the eastern fault, which is the western boundary fault of the Lower Main Valley (Figure 9).

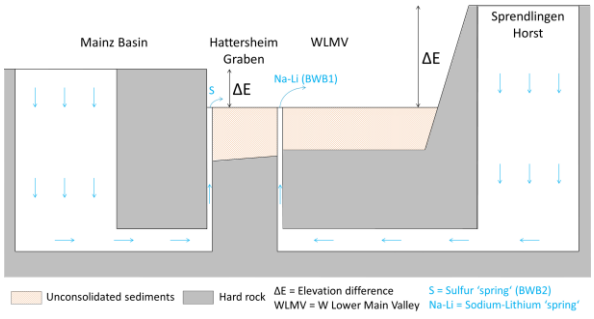

Figure 9: Hydraulic model for Bad Weilbach 'springs' (not to scale).

Both almost N-S striking faults are permeable at the sections with the springs (part of a pull-apart basin?), which is indicated by high mantle helium (^{3}He) concentrations (section 2.4). The different hydraulic head of the topography-driven system (Odin's Forest with higher elevated recharge area; Figure 9) is causing a higher velocity of the rising Na-Li spring fluid as evident by the higher Rn activity.

The mantle helium containing samples in the study area *sensu stricto* are characterized by low ^{222}Rn activities with exception of the two high-Rn samples GG25 and GG03, which are both located at the WMF.

Samples GG09 located in the north and GG13 in the east of the study area *sensu stricto* are characterized by slightly higher Rn activities around 4000 Bq/m^3. Monitoring well GG09 is situated already in the area of reduced thickness of the unconsolidated Quaternary sediments (<20 m) and in the convergence of the WMF and its synthetic fault which implies a high elevated basement in the subsurface. Also in case of GG13 the high elevated basement (Groß-Gerau Horst) is responsible for the slightly enhanced Rn activity.

Therefore, not only the existence of permeable structures but also the depth of the basement (where the water is "charged" with radon) is responsible whether the signal reaches the uppermost 10 m of the Quaternary aquifer. The transport duration is restricted to 10 days due to the short half-life time of ^{222}Rn to explain the decrease of the highest measured activity of 26,000 Bq/m^3 (highly permeable fault in hard rocks plus high elevation of basement) to the activity concentration of 4,000 Bq/m^3. After 20 days the lowest measured activity of 700 Bq/l is reached. At the latest after 38 days (10 half-life times) the radon signal cannot be detected anymore. Therefore only 10 days are available in the present case for the radon to convectively penetrate the hard rocks above the basement and to dispersively migrate through the unconsolidated Quaternary sediments of the ground-water aquifer.

The unconsolidated Quaternary sediments cannot convectively be penetrated because the fault does not cause an increase in permeability (no open fractures) in the loose sand and gravel.

In case of the permeable section of the synthetic fault (sample GG26), the basement is particularly deep seated within the Trebur Graben. The unconsolidated sediment thickness is >100 m. Therefore, radon is migrating around 15 days before reaching the uppermost groundwater.

In contrast to other geothermal areas worldwide, soil air measurements (helium and radon) in the northern URG are not suitable to detect fault traces directly at the earth's surface. This is caused by the extremely high abundance of the atmospheric component in the soil air in case of helium (Beck 2014) as well as the thickness of the local groundwater aquifer and its variable sediment composition in case of radon (Kuhn 2014).

2.4 Noble gas isotopic composition

Most samples in the study area consist of a mixture of crustal helium and air saturated water (ASW) and one group of samples is affected by a tritiogenic shift of the data points (see chapter 4).

However, one group of samples (including the two Bad Weilbach 'springs') is mainly representing mixtures of crustal and mantle helium. The missing of near-surface ASW and the presence of mantle helium is clearly indicating an upward migration from great depth.

In the map view (Figure 10) two permeable structures can be identified by positive mantle helium anomalies namely a section at the WBF and a section at the almost paralleling synthetic fault.

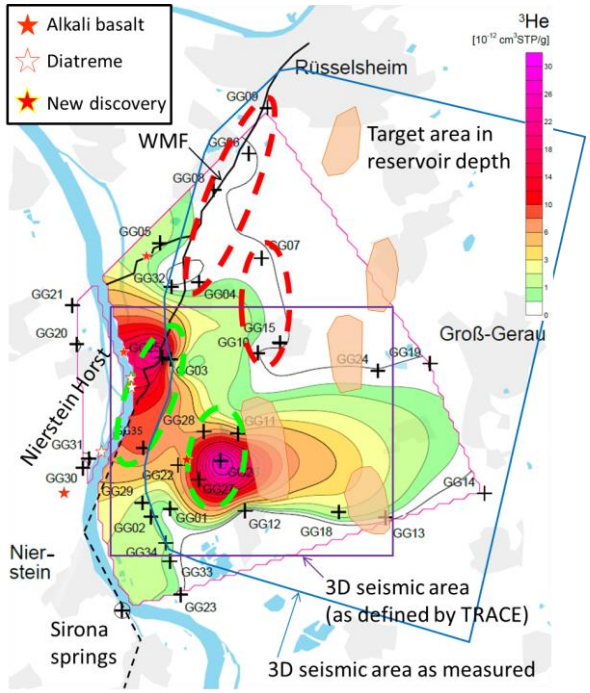

Figure 10: Map with interpolated mantle helium concentrations (Freundt et al. 2015, modified). Please note that the positive anomaly at the WMF apparently continues within the practically impermeable rocks of the Nierstein Horst (= artefact of the interpolation). The stars represent small alkali-basalt occurrences and diatremes (see Lutz et al. 2013). The basalt occurrence (yellow rim) in the area of the major positive anomaly near the synthetic fault was discovered during fieldwork by one of the coauthors (G. Schmidt).

Figure 10 also shows the areal extent of the 3D survey area and the target areas (mainly along the Nauheim-Wallerstätten fault system; not shown) as defined before implementation of the TRACE study.

2.5 Geomechanical modeling

The results of independent geomechanical modelling of the synthetic fault are shown in Figure 11.

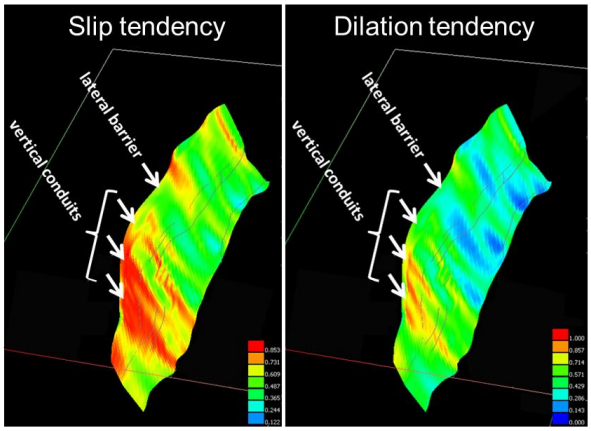

Figure 11: Geomechanical modelling of the synthetic fault (Reinecker, unpublished).

Please note that the zone in Figure 10 characterized by highest mantle helium concentrations (around sample GG26) is located exactly at the section with highest slip and dilation tendency (red vertical channels) shown in Figure 11. The samples without mantle helium (GG10, GG15, GG07; Figure 10) are represented by low slip and dilation tendency (blue lateral barriers; Figure 11).

3. CONCEPTUAL MODEL

The conceptual model is shown in Figure 12.

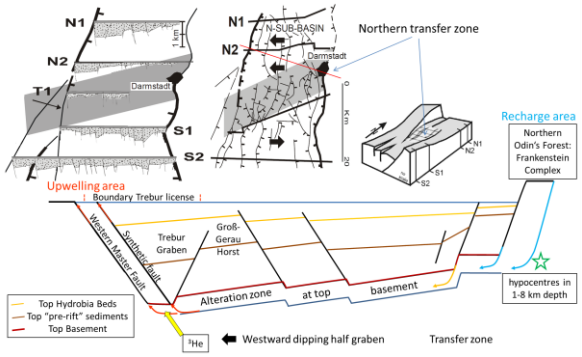

Figure 12: Conceptual model. Structures schematic after Derer 2003 (see text for explanation).

The major recharge of meteoric water occurs at the graben shoulder in the area of the northern crystalline Odin's Forest (Frankenstein Complex). Hypocenters of most recent earthquake activity in 1-8 km depth point to currently permeable (i.e. active) fault zones in that area which allow infiltration in deep zones of the crystalline basement. In contrast, the runoff from the graben shoulder (not shown) delivers the major portion of the recharge for the shallow Quaternary groundwater aquifer in the URG. The flow path of the deep water is mainly within the alteration zone at the top of the basement in western direction in the westward dipping half graben. During descent and along the flow path the meteoric water is heating up and by fluid-rock interaction (mainly with granodiorite) the fluid receives its NaCl-dominated salinity especially via mobilization of fossil sea water. The practically impermeable lowermost Permo-Carboniferous stratigraphic unit prevents a rise of the saline fluid. Also inactive fault zones are sealed with precipitated minerals and do not allow for upwelling of the brine any more (self-sealing effect). Only in the area of the western master fault an upwelling is possible once permeable structures are reached. The convectively rising hot reservoir fluid causes a slightly enhanced geothermal gradient in the uppermost earth crust which is not as pronounced as in Soultz and Landau regions (Figure 15; red-orange areas). The topographic driving force results from the elevation difference of the recharge area in the mountains compared to the low elevated upwelling area in the Upper Rhine valley. Minor driving forces might result from buoyancy of the hot brine and in the uppermost section also by CO_2 degassing (gas lift) because beside mantle helium also mantle CO_2 (from the mantle shear zone; Figure 13) is added to the saline fluid.

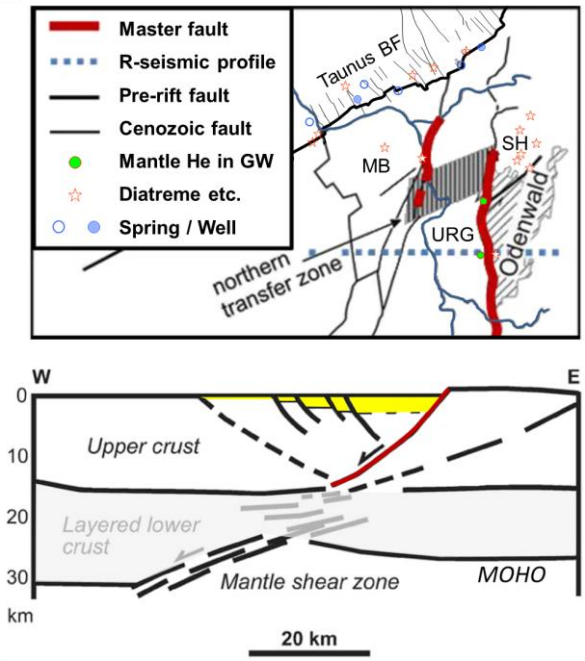

Figure 13: Mantle shear zone as revealed by refraction seismic profiles (Baillieux et al. 2012, modified with compiled data of Böcker et al. 2016, Bauer et al. 2010 and He data of Friedrich 2007).

The rise of the brine is fast (see section 2.3) compared to the slow velocity along the flow path. This holds true for the fault section in hard rocks. As soon as the fluid reaches the Plio-Pleistocene unconsolidated sediments, a massive mixing with shallow groundwater and a slow dispersive movement up to a few meters below the earth surface takes place in the area of the master fault and its almost paralleling synthetic fault. The diluted (still denser) brine is progressively layered over by young meteoric water to the east.

Due to the significant residence time during migration of the fluid to the west, it is most likely that chemical equilibrium between granodiorite and fluid was achieved. Additionally, a complication in fluid evolution is the dissolution of Oligocene salt. The dissolution process must not necessarily be related to salt from the Oligocene sediments (mid-Cerithia beds) but could also be related to halite coatings in the crystalline basement derived from infiltrated Oligocene seawater. The small portion in samples GG25 and GG26, which indicate the major upwelling zones, show that the upwelling in the high-permeable fault sections occurred rapidly. In contrast, sample GG08 without mantle helium (Figure 10) and highest portion of dissolved Oligocene salt (Figure 5) is indicating a low-permeable section at the WMF.

4. DISCUSSION OF APPLIED ASPECTS

The TRACE approach is a further development of former exploration strategies developed in the East African Rift System (EARS; e.g. Kraml et al. 2007) and the Basin & Range Province (Preuss 2007). Those strategies already resulted in the identification of promising geothermal resources. Due to the rare occurrence of surface manifestations in Germany, the TRACE approach is based (in contrast to those former applications) on groundwater samples from easy accessible and nationwide available monitoring wells.

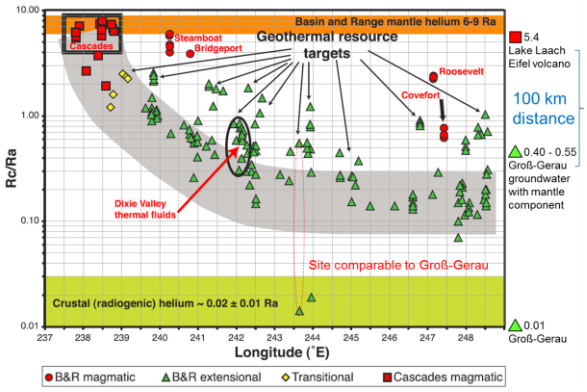

Figure 14: Comparison with Basin & Range Province, U.S.A. (Kennedy & van Soest 2007). R/Ra of Lake Laach from Aeschbach-Hertig et al. (1996) and R/Ra of Groß-Gerau (this study)

The interpretation of groundwater samples is more complex than those of surface manifestations (hot springs) due to the more pronounced dilution of the mantle helium tracer signal with groundwater. The sampling strategy of the TRACE approach is more complex because it has to be individually adapted to the local conditions, i.e. array in uppermost aquifer versus smaller number of deep groundwater wells located close to the fault trace. The groundwater flow direction and velocity has to be considered in planning the sampling campaign as well as in interpreting the data. In case of hydrochemistry and radiogenic isotope data of shallow groundwater ("array samples") also anthropogenic contamination has to be figured out.

The lower groundwater aquifer is not significantly affected by anthropogenic effects and thus allows for a less complex evaluation of the chemistry and radiogenic isotope data from deep groundwater wells.

Helium isotope data of shallow "array samples" are not affected by any chemical contamination. They are only affected by tritium released by nuclear power plants or remains from nuclear weapon tests in the late 1950's and early 1960's. The occurrence of tritium in the water sample can easily be proven e.g. with beta-spectrometric measurements and the data shift in ^{3}He, caused by the decay of tritium identified accordingly. Already the deeper part of the uppermost aquifer and the lower aquifer are practically tritium-free.

Currently, the TRACE approach is able to qualitatively assess fault sections concerning their permeability in depth. The next step will be the half-quantitative calibration of the mantle helium content and related fracture permeability considering regional background values (Figure 15). Those background R/Ra values are 0.1-0.3 in the central URG (shear zone) and R/Ra = 1.4-1.7 in the southern URG around Kaiserstuhl volcanic complex (Figure 15).

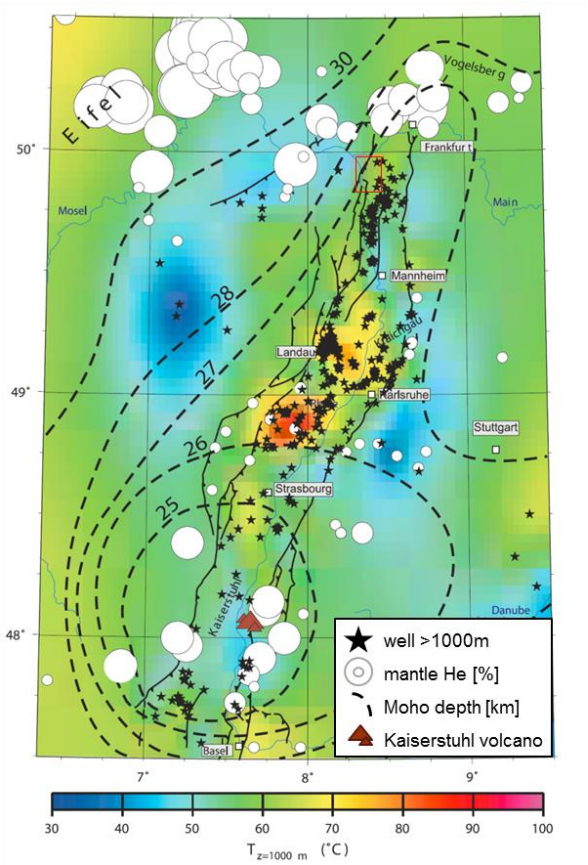

Figure 15: Regional background values of ^{3}He showing Eifel, Taunus border fault, and URG (Clauser et al. 2002, modified). Please note the lack of data in the northern URG around the study area (red rectangle).

The activity of Kaiserstuhl volcanic complex lasted from 18-16 Ma (Kraml et al. 1996) but its conduits and numerous surrounding older dikes, necks etc. (Keller et al. 2002) are reflecting the shallow MOHO depth (Dèzes et al. 2004) and the frequent penetration of the entire crust by mantle melts, mainly during Tertiary times of major graben formation. Nowadays, those conduits still allow for the ascent of mantle fluids up to the earth's surface (the latter only if permeable structures still exist in the upper crust). These findings of mantle helium in the non-magmatic URG rift are comparable to the extensional setting of the Basin & Range province, U.S.A. (Figure 14; Kennedy & van Soest 2007) and the non-magmatic sections of the western branch of the EARS (Kraml et al. 2016, accepted). Typical R/Ra ratios are between 0.2 and 0.3 for saline hot springs representing upwelling basement fluids along permeable faults in Tanzania (Kraml et al. 2016, accepted) and 0.1-0.2 considering unpublished data from Uganda (Kraml et al. 2007) and Rwanda (Jolie & Kraml 2008).

5. CONCLUSIONS

The TRACE approach allows for identification of deep-reaching permeable fault zone sections via low-budget tracer analyses independent of (and prior to) 3D seismic data acquisition and -evaluation (→ conceptual model and not only a geological model of the subsurface).

The anomalies in mantle helium (and chlorine; Al Najem et al. 2016) yielded a significantly higher spatial resolution concerning allocation to individual faults than former investigations based on resistivity methods (Schmitt & Steuer 1974; Siemon et al. 2001). The presented results for the first time allow to also assess the role of the synthetic fault in fluid flow additional to the known upwelling at the WMF.

This study's sampling approach can only be chosen in case of known salt water anomalies in the uppermost groundwater, like in Groß-Gerau (northern URG, Siemon et al. 2001) or Ohlsbach (southern URG, Stober et al. 1999). In all other cases deep wells reaching the lower groundwater have to be sampled. The latter is separated via impermeable clay layers from the upper groundwater in the URG.

Radon measurements of water samples (especially of springs) deliver valuable insights into migration velocities at fault zones and could allow to half-quantitatively assess the permeability in the subsurface in combination with mantle helium concentrations in the future.

The bigger the data base will be by analyzing further helium isotope samples, the better the envisaged half-quantitative calibration via regional background values will be (compare Wiersberg & Erzinger 2011).

Of additional interest would be to investigate whether comparatively weak earthquakes (like the 2014 M=4 events) are already able to modify fault-related flow paths and their permeability, as observed in the EARS in case of stronger earthquakes (Kraml et al. 2007).

The consideration of surface manifestations (also in case they are sparse) is valuable because e.g. the known mineralization is a natural analogue of the scaling process. In case no mitigation measures are taken, this process would take place in the planned power plant via decompression and related CO_2 degassing (calcite scaling in the production well) as well as cooling at the heat exchanger causing scales of mixed sulfides (Degering et al. 2013).

Additional advantages of the TRACE approach are:

- Risk mitigation in yielding economically viable flow rates in the drilling and testing phase of the first exploration well, i.e. a positive "TRACE result" could even convince insurance companies for ensuring the geological risk.
- Optimization of 3D seismic survey designs to ensure coverage of promising target fault sections (Figure 10).
- Potential cost reduction by narrowing down the extension of cost-intensive 3D seismic surveys (60% in the present case; Figure 10).

REFERENCES

Aeschbach-Hertig W., Kipfer, R., Hofer, M., Imboden, D. M., Wieler R. and Signer P.: Quantification of gas fluxes from the subcontinental mantle: The example of Laacher See, a maar lake in Germany, *Geochim. Cosmochim. Acta*, ***60***, (1996), 31–41.

Al Najem, S., Freundt, F., Schmidt, G., Rheinberger, S., Kraml, M., Aeschbach, W. and Isenbeck-Schröter, M.: Salinization of shallow groundwater by a deep fluid ascending at the western main fault zone of the northern Upper Rhine Graben, Germany: Discussion of the origin and evolution using major and trace element compositions. *Submitted to Applied Geochemistry*, (2016).

Baillieux, P., Schill, E., Moresi, L., Abdelfettah, Y. and Dezayes, C.: Investigation of Natural Permeability in Graben Systems: Soultz EGS Site (France), *Proceedings, Thirty-Seventh Workshop on Geothermal Reservoir Engineering January 30 - February 1*, Stanford University, Stanford, California, (2012), SGP-TR-194, 12 pages

Bauer, W. Becker, A. and Schwarz, M.: Geothermal Greenfield Exploration – an Example from the Taunus Area, Germany, *ERDÖL ERDGAS KOHLE* **126(2)**, (2010), 64-67.

Beck, B.: Lokalisierung von aktiven geologischen Störungszonen im Oberrheingraben durch Messung von $^{3}He/^{4}He$-Verhältnissen in der Bodenluft. *Diplomarbeit Universität Heidelberg*, Heidelberg, (2014), 151 pages.

Böcker, J., Littke, R. and Forster, A.: An overview on source rocks and the petroleum system of the central Upper Rhine Graben. *Int J Earth Sci*, (2016), DOI 10.1007/s00531-016-1330-3.

Böger, K.: Botanisches Gutachten zu den geplanten Naturschutzgebieten Salzquelle von Trebur und Herrenwiese-Fischerpfad von Astheim als Teile des Gutachtens über das Landschaftsschutzgebiet Schwarzbachaue von Trebur, Gutachten, Darmstadt, (1985), 80 pages

Bucher, K. and Stober, I.: Fluids in the upper continental crust, *Geofluids*, **10**, (2010), 241-253.

Bucher, K., Zhu, Y. and Stober, I.: Groundwater in fractured crystalline rocks, the Clara mine, Black Forest (Germany), *Int J Earth Sci*, **98**, (2009), 1727-1739.

Carlé, W.: Die Mineral- und Thermalwässer von Mitteleuropa – Geologie, Chemismus, Genese. *Wissenschaftliche Verlagsgesellschaft mbH*, Stuttgart, (1975), 643 pages.

Clauser, C., Griesshaber, E. and Neugebauer, H. J.: Decoupled thermal and mantle helium anomalies: Implications for the transport regime in continental rift zones, *Journal of Geophysical Research*, **107 No. B11, 2269**, (2002), doi:10.102 9/2001JB000675, 2002.

Degering, D., Köhler, M. and Fleischer, K.: Bilanzierung und Entsorgung radioaktiver Rückstände aus Geothermieanlagen, *Proceedings of Der Geothermiekongress 2013*, 12.-14. November 2013, Essen, Germany, (2013).

Derer, C. E.: Tectono-Sedimentary Evolution of the Northern Upper Rhine Graben (Germany), With Special Regard to the Early Syn-Rift Stage. *Dissertation, Universität Bonn*, (2003), 99 pages.

Dèzes, P., Schmid, S. M. and Ziegler, P. A.: Evolution of the European Cenozoic Rift System: interaction of the Alpine and Pyrenean orogens with their foreland lithosphere, *Tectonophysics*, **389(1-2)**, (2004), 1-33.

Freundt, F., Al Najem, S., Schmidt, G., Aeschbach-Hertig, W., Isenbeck-Schröter, M. and Kraml, M.: Application of helium isotopes in shallow groundwater for geothermal exploration in the Upper Rhine Graben, *25th Goldschmidt Conference Abstract, August 16-21, 2015*, Prague, Czech Republic, (2015), poster contribution

Friedrich, R.: Grundwassercharakterisierung mit Umwelttracern: Erkundung des Grundwassers der Odenwald-Region sowie Implementierung eines neuen Edelgas-Massenspektrometersystems, *Dissertation, Universität Heidelberg*, Heidelberg, (2007), 272 pages.

Homuth, B., Rümpker, G. and Kracht, M.: Natürliche Seismizität im nördlichen Oberrheingraben – bisherige Ergebnisse des Projektes SiMoN, 9. *Tiefengeothermieforum Hessen*, September 30, 2014, Darmstadt, Germany, (2014).

Jolie, E. and Kraml, M.: Geothermal Potential Assessment in the Virunga National Park, Rwanda. EGU Conference Vienna 13-18 April 2008, *Geophysical Research Abstracts*, Vol. 10, EGU2008-A-12141, (2008).

Keller, J., Kraml, M. and Henjes-Kunst, F.: $^{40}Ar/^{39}Ar$ single crystal laser dating of early volcanism in the Upper Rhine Graben and tectonic implications, *Schweiz. Mineral. Petrogr. Mitt.*, **82**, (2002), 121-130.

Kennedy, B. M. and van Soest, M. C.: Flow of Mantle Fluids Through the Ductile Lower Crust: Helium Isotope Trends, *Science*, **318**, (2007), 1433-1436.

Korte, E., Kalbhenn, U., Berg, T. and Hennings, R.: Fischökologische Untersuchung in den Fließgewässersystemen der Untermainebene unter besonderer Berücksichtigung der Fischarten des Anhangs II der FFH-Richtlinie, Studie, (2007), 71 pp

Kraml, M. et al.: Detailed surface analysis of the Buranga geothermal prospect, West-Uganda. *BGR draft terminal report*, (2007), 168 pages.

Kraml, M., Kaudse, T., Aeschbach, W. and Tanzanian Exploration Team: The surge for volcanic heat sources in Tanzania: A helium isotope perspective, *Proceedings, 6th African Rift*

Geothermal Conference 2nd – 4th November 2016, Addis Ababa, Ethiopia, (2016, accepted).

Kraml, M., Keller, J. and Henjes-Kunst, F.: Spot Fusion and Incremental Heating of Single Crystals from Kaiserstuhl Volcanic Rocks with the BGR $^{40}Ar/^{39}Ar$ Laser Probe, *V. M. Goldschmidt Conference March 31 - April 4, 1996*, Heidelberg, Germany, (1996), Journal of Conference Abstracts Volume 1(1): 332.

Kuhn, G.: Radonmessungen in der Bodenluft bei Trebur einschließlich der Entwicklung eines standardisierten Messverfahrens zur Lokalisation von Verwerfungen, *Masterarbeit Technische Universität Darmstadt*, (2014), 100 pages.

Kulaksız, S. and Bau, M.: Contrasting behaviour of anthropogenic gadolinium and natural rare earth elements in estuaries and the gadolinium input into the North Sea, *Earth and Planetary Science Letters*, **260**, (2007), 361-371.

Landsberg, H.: Der Erdbebenschwarm von Groß-Gerau 1869-1871. Gerlands Beiträge zur Geophysik, (1931).

Lutz et al.: Buried Paleogene Maar-Diatreme Volcanoes within the northern Upper Rhine-graben, Germany, (2016, in prep.).

Lutz, H., Lorenz, V., Engel, T., Häfner, F. and Haneke, J.: Paleogene phreatomagmatic volcanism on the western main fault of the northern Upper Rhine Graben (Kisselwörth diatreme and Nierstein-Astheim Volcanic System, Germany), *Bull Volcanol*, **75**, (2013), 741

Markl, G. and Bucher, K.: Composition of fluids in the lower crust inferred from metamorphic salt in lower crustal rocks, *Nature*, **391**, (1998), 781-783

McLennan, S. M.: Rare Earth Elements in Sedimentary Rocks: Influence of Provenance and Sedimentary Processes, in: Geochemistry and Mineralogy of Rare Earth Elements, Lipkin, B. R., and McKay, G. A. (Eds.), *Reviews in Mineralogy 21*, (1989), 169-200.

Preuss, P.: Helium Isotopes Point to New Sources of Geothermal Energy, (2007), (website visited on 30.07.2015) http://www2.lbl.gov/Science-Articles/Archive/ESD-geothermal-energy.html

Schäfer, P.: Mainzer Becken. Stratigraphie – Paläontologie – Exkursionen. Sammlung Geologischer Führer Band 79, 2. völlig neu bearbeitete Auflage, *Gebr. Bornträger*, Stuttgart, (2012), 333 pages.

Schmidt, G., Al Najem, S., Isenbeck-Schröter, M., Freundt, F., Kraml, M. Eichstädter, R. and Aeschbach, W.: Ascending deep fluids into shallow aquifer at hydraulically active segments of the Western Boundary Fault of the Rhine Graben, Germany: Constraints from $^{87}Sr/^{86}Sr$ ratios, *Proceedings of 15th Water-Rock Interaction International Symposium, WRI-15, 16 to 21 October 2016*, Évora, Portugal, (2016).

Schmitt, O. and Steuer, A. et al.: Erläuterungen zur Geologischen Karte von Hessen 1:25000, Blatt 6016 Groß Gerau 2nd Edition, Wiesbaden, (1974), 202 pages.

Schmitt, O.: Zum Verlauf der westlichen Randverwerfung des zentralen Oberrheingrabens zwischen dem Rhein südlich Nackenheim und dem Main bei Rüsselsheim sowie über eine Grundwasserkaskade und Bauschäden im Bereich dieser Störungszone, in: Approaches to Taphrogenesis - Proceedings of an International Rift Symposium in Karlsruhe April 13-15, 1972, Illies, J. H., Fuchs, K. (Eds.), (1974), 254-260.

Schwabe, J. and Scheibe, R.: Groß-Gerau: Gravimetrie-Survey und Modellierung im Zuge des Projektes "Geothermie" der ÜWG GmbH. – Unveröffentlichte Studie, Geophysik GGD mbH Leipzig, (2012), 29 pages.

Siemon, B., Blum, R., Pöschl, W., Voß, W.: Aeroelektromagnetische und gleichstromgeoelektrische Erkundung eines Salzwasservorkommens im Hessischen Ried, *Geol. Jb. Hessen*, **128**, (2001), 115-125.

Stober, I. and Bucher, K.: Origin of salinity of deep groundwater in crystalline rocks, *Terra Nova*, **11**, (1999), 181-185.

Stober, I., Richter, A., Brost, E. and Bucher, K.: The Ohlsbach Plume – Discharge of deep saline water from the crystalline basement of the Black Forest, Germany, *Hydrogeology Journal*, **7**, (1999), 273-283.

Vaselli, O., Minissale, A., Tassi, F., Magro, G., Seghedi, I., Ioane, D. and Szakacs, A.: A geochemical traverse across the Eastern Carpathians (Romania): constraints on the origin and evolution of the mineral water and gas discharges, *Chemical Geology*, **182**, (2002), 637-654.

Wiersberg, T. and Erzinger, J.: Chemical and isotope compositions of drilling mud gas from the San Andreas Fault Observatory at Depth (SA FOD) boreholes: Implications on gas migration and the permeability structure of the San Andreas Fault, *Chemical Geology*, **284**, (2011), 148-159.

Acknowledgements

We thank the Federal Ministry for Economic Affairs and Energy (funding code FKZ: 0325390) for financial support, the HLNUG for support in sampling and data provision, and the Li isotope laboratory in Frankfurt University, Germany, namely H.-M. Seitz, for enabling the measurements. Last but not least we thank Tobias Hochschild (GeoT) for his support during 3D seismic data evaluation and Andreas Wunsch for literature research.